J. Fluid Mech. (2013), *vol.* 737, *pp.* 232–248.
doi:10.1017/jfm.2013.540

The velocity of 'large' viscous drops falling on a coated vertical fibre

Liyan Yu† and John Hinch

Department of Applied Mathematics and Theoretical Physics, University of Cambridge, Wilberforce Road, Cambridge CB3 0WA, UK

(Received 8 April 2013; revised 24 September 2013; accepted 7 October 2013; first published online 25 November 2013)

Kalliadasis & Chang (*J. Fluid Mech.*, vol. 261, 1994, pp. 135–168) showed within lubrication theory that if a liquid film is thicker than a critical value then drops will accelerate and grow, whereas with thinner films the drops fall at a constant velocity. As the thickness of the film increases to the critical value, the drops move faster and are larger. We revisit their asymptotic analysis of these large drops. While we recover their results for the leading-order and first correction, we do not agree on further corrections. In particular we find it necessary to evaluate the third correction, which they do not consider, before we obtain a first approximation to the dependence of the speed on the non-dimensional control parameter. We proceed to two further corrections in order to improve this first approximation to the speed.

Key words: interfacial flows (free surface), solitary waves, thin films

1. Introduction

A cylinder of liquid suffers a Rayleigh–Plateau instability in which surface tension reduces the surface area, turning the cylinder into spherical drops. The wavelength of the instability is the circumference of the cylinder. The time scale of the instability depends on whether the driving force of surface tension is resisted by inertia or viscosity. We are interested in viscously dominated dynamics.

A thin liquid film on a fibre cannot become spherical drops because the fibre is in the way. Instead, without gravity, the liquid film rearranges, with a similar wavelength, into bulges in the film no more than four times as thick as the initial thickness (Hammond 1983). There is then a slow development process in which the higher pressure in smaller bulges feeds growing larger bulges.

On a vertical fibre gravity must be considered. The appropriate non-dimensional measure is a reduced Bond number, reduced to take account of the film being thin,

$$G = \frac{\rho g a^3}{\gamma h_0}, \tag{1.1}$$

where ρ is the density of the liquid, g the acceleration due to gravity, a the radius of the fibre, γ the surface tension and h_0 the undisturbed film thickness. Quéré (1990) found in experiments that there was a critical value of $G = 0.71$ separating two different behaviours. For small G, i.e. for films thicker than a critical value, Quéré

† Email address for correspondence: liyan.yu@cantab.net

found that the bulges grew to become large drops as they fell down the fibre, while for large G, i.e. for thinner films, the bulges fell with a steady shape.

Kalliadasis & Chang (1994) used the lubrication approximation to study the behaviour. They found the critical value of the reduced Bond number to be $G = 0.595$. In numerical solutions of the lubrication equations for smaller G, they saw small bulges grow to a very large size in a finite time, with a suggested $(t_* - t)^{-1/3}$ blowup. Later Chang & Demekhin (1999) found the correct form of the blowup to be $(t_* - t)^{-2}$, due to the bulges leaving behind thinner films than the film in front. At large G, Kalliadasis & Chang (1994) found numerically that an initial disturbance developed into a train of solitary waves, each with the same amplitude and speed. The amplitude and speed became large as G decreased towards its critical value. Kalliadasis & Chang went on to present an asymptotic analysis of these large solitary waves within the lubrication approximation. We shall revisit their analysis in this paper, correcting some details and adding extra terms. Our result for the key dependence of the speed of the waves on the value of G differs significantly from that of Kalliadasis & Chang. We discuss the differences in our calculations at the end of the paper.

The critical value of $G = 0.595$ is near to the transition in linear instability at $G = 0.5407$ found by Duprat *et al.* (2007) for the change from convective to absolute instability. It is unclear how this transition is relevant to the behaviour of the large-amplitude solitary waves.

Experiments have often been conducted with relatively thick films of liquid coating the fibres. Kliakhandler, Davis & Bankoff (2001) introduced a model equation which incorporates into the standard lubrication equations the full nonlinear expression for the curvature of the free surface and an expression for the flux of an axial flow driven by gravity in a film whose thickness is comparable to the radius of the fibre. This model equation has been employed by a number of groups (Craster & Matar 2006), Duprat *et al.* (2007) and Smolka, North & Guerra (2008). The model equation is asymptotically correct for disturbances with a length scale much longer than the radius of the fibre. Unfortunately, the instability of interest has a wavelength comparable with the radius of the fibre. We shall work entirely within the lubrication approximation.

2. Governing equations

We consider a solid vertical fibre of radius a coated by an axisymmetric film of a viscous liquid of thickness $h(x, t)$, where x measures axial position downwards along the fibre, see figure 1. The film is assumed to be both thin $h \ll a$ and vary along the fibre on the length scale of the fibre radius, so $|\partial h/\partial x| \ll 1$. The capillary pressure in the film is to a first approximation γ/a, where γ is the surface tension. This constant pressure drives no flow. The flow is driven by small $O(\gamma h/a^2)$ corrections, which vary along the fibre, and which are typically negative corresponding to the film radius being the larger $a + h$ rather than a. We shall ignore the leading-order constant and instead call the first correction 'the capillary pressure'. Thus in the thin-film approximation our capillary pressure will be

$$p = \gamma(-h/a^2 - h_{xx}). \tag{2.1}$$

The gradient of this pressure along with gravity drives a flow down the fibre. For a thin film, the lubrication approximation to this flow gives a flux per unit circumference

$$q = \frac{h^3}{3\mu}(\rho g - p_x), \tag{2.2}$$

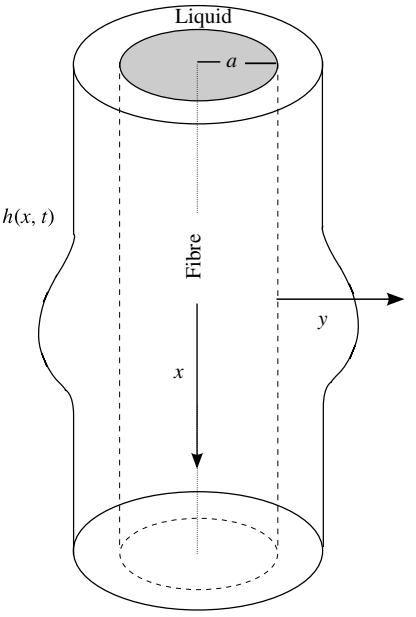

FIGURE 1. Sketch of the geometry.

where μ is the viscosity. Finally, mass conservation is

$$h_t + q_x = 0. \tag{2.3}$$

We non-dimensionalize the axial position x by the radius of the fibre a, the film thickness $h(x,t)$ by an assumed initial uniform thickness h_0, time t by the time scale of the viscous instability $3\mu a^4/\gamma h_0^3$, and capillary pressure by $\gamma h_0/a^2$. With this non-dimensionalization, the governing equation becomes

$$h_t + \left(h^3(G + (h + h_{xx})_x)\right)_x = 0, \tag{2.4}$$

with the single non-dimensional parameter the reduced Bond number $G = \rho g a^3/\gamma h_0$, an effective strength of gravity.

We are interested in solitary waves which propagate steadily at speed c without change of form, i.e. in solutions of the form $h(x-ct)$. Substituting this into (2.4) above and henceforth relabelling $x - ct$ as x, integrating once and applying the condition of the initial thickness far from the disturbance, we obtain

$$-ch + h^3(G + (h + h_{xx})_x) = -c + G \quad \text{with } h \to 1 \text{ as } x \to \pm\infty. \tag{2.5}$$

We seek solutions of this equation. It is an eigenvalue problem, to find the eigenvalue of the speed for given Bond number $c(G)$ and the associated eigensolution for the shape $h(x)$. Note that the velocity c has been non-dimensionalized by $\gamma h_0^3/3\mu a^3$.

3. Numerical results

A numerical solution of the nonlinear third-order differential equation (2.5) has been found with a combination of iterating unknown values of some parameters and shooting inwards from the far field on either side of the solitary wave to a common meeting point. The meeting point was chosen to be where $h_{xx} = 0$, $h_x < 0$ and h was

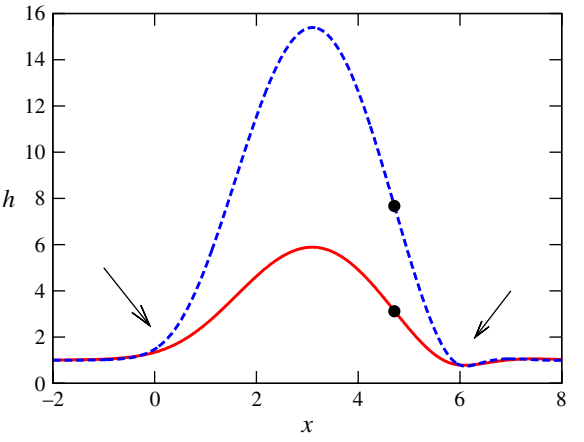

FIGURE 2. (Colour online) The shape of solitary waves $h(x)$. The lower continuous curve is for $G = 0.7$ with $c = 14.2$ while the upper dashed curve is for $G = 0.63$ with $c = 47.7$. The filled circles denote the patching point $x = 3\pi/2$. The arrows point to the transition regions from the main drop to the uniform film in front of and behind the wave.

suitably greater than 1, say $h > 1.5$. When the parameters have the wrong values, the solutions to the left of the meeting point have different values of h and h_x from those to the right.

In the far field, (2.5) can be linearized around the undisturbed thickness $h = 1$. For $c > 3G$, which it is always found to be, there is one linearized solution which grows exponentially as x increases, and there are two linearized solutions which oscillate and grow exponentially as x decreases. For the solution to the left of the meeting point, i.e. above the falling drop, we start by setting h, h_x and h_{xx} corresponding to the one linearized solution which grows exponentially with increasing x, starting at a very small amplitude. For the solution to the right, i.e. below the falling drop, we start with a combination of the two solutions which grow as x decreases, the ratio of the two different solutions being a free parameter. This free parameter and the unknown speed c are adjusted iteratively until the solutions from the left and the right meet with h and h_x equal.

Figure 2 plots the solitary waves for $G = 0.63$ and $G = 0.7$. The solitary wave is localized in the region $[0, 2\pi]$ and the meeting point has been shifted to $x = 3\pi/2$, both for reasons which will become apparent in the next section. The amplitude increases as G decreases. The wave with the higher amplitude decays more rapidly into the far field.

Figure 3 plots as functions of the reduced Bond number G the speed c and the amplitude h_{max} defined to be the maximum value of $h(x)$. There are no solutions for G below a critical value of $\sim$0.6. The speed and the amplitude increase without limit as G decreases to the critical value. The amplitude decreases monotonically as G increases from the critical value. On the other hand, the speed c decreases to a minimum of 6.3 around $G = 1.1$ before increasing approximately linearly at large G. In fact, an asymptotic analysis shows that c increases as $3G + 1.216$ when G is large. For $G < 0.9$, the drop is large enough for there to be a recirculation zone. Near $G = 0.9$ the recirculation region is just near the maximum thickness of the drop. As G decreases to its critical value, most of the large drop is recirculating.

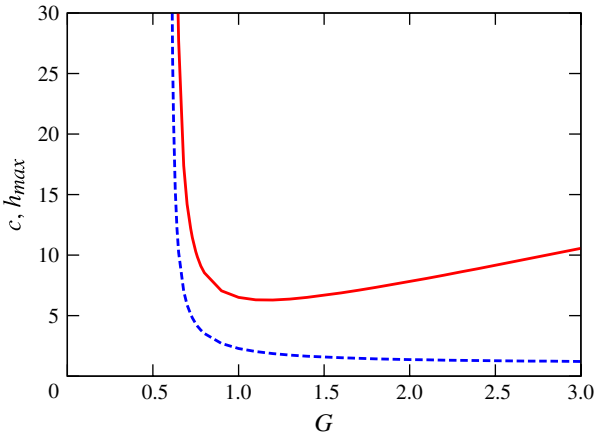

FIGURE 3. (Colour online) Solitary waves. The upper continuous curve gives the speed c as a function of the reduced Bond number G, while the lower dashed curve gives the maximum of $h(x)$ as a function of G.

4. First approximations

In this section, we will obtain the leading approximation to solutions of (2.5) for fast large-amplitude solitary waves. This will lead us to follow Kalliadasis & Chang (1994) and pose a matched asymptotic solution in terms of the small parameter $c^{-1/3}$. We shall need to go to the third correction before the problem becomes fully resolved and we find an approximation to the relation between G and c.

When h is large, the h^3-factor in the flux q of lubrication theory produces a large flux that cannot be balanced unless the pressure gradient nearly balances gravity. We therefore deduce that the capillary pressure has approximately a hydrostatic variation. This $O(1)$ variation is, however, small compared with the potential $O(h)$ variation when h is large. Thus to the leading order, there is a large constant capillary pressure $-\kappa_0$ where $h(x)$ is large. Hence (for drops smaller than the radius of the fibre)

$$h(x) \sim \kappa_0(1 - \cos x), \tag{4.1}$$

where we have chosen the region where h is large to run from $x = 0$ to $x = 2\pi$. We note in figure 2 that the region where h is large is the same for the two waves plotted and is approximately 2π long. As h reduces from large values, it takes a parabolic shape

$$h(x) \sim \tfrac{1}{2}\kappa_0(x - x_0)^2, \tag{4.2}$$

where $x_0 = 0$ at the trailing left-hand side above the falling drop, and $x_0 = 2\pi$ at the leading right-hand side below the falling drop.

At the two ends of the large drop, near to $x = 0$ and 2π, the capillary pressure must change from its large value $-\kappa_0$ in the drop to the value -1 in the uniform film. This change occurs in a short transition region first investigated by Bretherton (1961) for bubbles advancing along a tube filled with a viscous liquid. Bretherton showed that when $h = O(1)$ it is possible for the large c terms in (2.5) to be balanced if there are variations in x on the short scale $c^{-1/3}$. With the rescaling

$$x = x_0 + c^{-1/3}\xi, \tag{4.3}$$

the governing equation (2.5) becomes at leading-order Bretherton's equation

$$h_{\xi\xi\xi} = \frac{h-1}{h^3}. \tag{4.4}$$

As discussed for the numerical solutions in the previous section, one considers the linearized behaviour in the approach to the uniform film $h \to 1$, finding disturbances like

$$\mathrm{e}^{\xi}, \quad \mathrm{e}^{-\xi/2}\cos\sqrt{3}\xi/2 \quad \text{and} \quad \mathrm{e}^{-\xi/2}\sin\sqrt{3}\xi/2. \tag{4.5}$$

The first solution is used for the far-field boundary conditions as $\xi \to -\infty$ in the left-hand transition region near to $x = 0$, while a combination of the second and third solutions is used for $\xi \to \infty$ in the right-hand transition region near to $x = 2\pi$.

Solving Bretherton's equation numerically in the two transition regions, one finds that as h becomes large as one enters the large drop, that is as $\xi \to +\infty$ for the left-hand transition region and as $\xi \to -\infty$ in the right-hand transition region,

$$h \sim \tfrac{1}{2}P_{\pm}\xi^2 + Q_{\pm}\xi + R_{\pm}. \tag{4.6}$$

Adjusting the amplitude of the single solution in the far field of the left-hand transition region, which is equivalent to an origin shift in ξ, one can make the linear term vanish, $Q_+ = 0$. Then $P_+ = 0.6430$ and $R_+ = 2.8996$. Matching the above quadratic behaviour leaving the left-hand transition region with the quadratic behaviour found before at the left-hand side of the large drop, we find a relationship between the capillary pressure $-\kappa_0$ in the large drop and its speed c

$$\tfrac{1}{2}P_+c^{2/3} = \tfrac{1}{2}\kappa_0. \tag{4.7}$$

In the far field of the right-hand transition region, there are two amplitudes for the two linearized solutions. Adjusting these two, one can again make the linear term vanish, $Q_- = 0$, and that leaves one degree of freedom so that R_- will vary as P_- varies. Now the coefficient of the parabolic shape at the left-hand side of the large drop, $\kappa_0/2$, is the same as that at the right-hand side, and so we require $P_- = P_+$. Adjusting the last degree of freedom in the far field to force P_- to take this value, one finds $R_- = -0.8453$. As P_+ and P_- are equal, we hereafter drop the subscripts.

To check the first approximations derived above, we have plotted the numerical solutions for the solitary waves using the predicted scalings. In figure 4, we divided the computed shape $h(x)$ by $c^{2/3}$ using the computed speed c, for three different values of G. We see that the rescaled shapes are very similar and that the maxima of 1.201, 1.233 and 1.270 are tending to the predicted value of $h_{max} = 2\kappa_0 = 2Pc^{2/3} = 1.286c^{2/3}$ as G decreases to the critical value. A more revealing way to look at the approach to the asymptotic limit is to calculate $h(\pi) - 2Pc^{2/3}$, which takes values $= -1.497$, -1.473, -1.443 as G decreases. We will return to these values later when we have corrections to the leading approximations. In figure 5 we plot the shape h as a function of the stretched variable ξ for the right-hand transition region below the falling drop. The curves from the three different values of G superpose well, showing that the stretched variable is appropriate.

Figure 6 shows the variation of the pressure within the solitary wave for $G = 0.61$. In the uniform films before ($x < -2$) and ahead ($x > 9$) of the wave, the capillary pressure is -1. In the interior of the large drop ($1 < x < 5$), the pressure is roughly constant with a value around -17.5, which should be compared with our first prediction of $-\kappa_0 = -Pc^{2/3} = -18.1$, using the computed value of $c = 149.6$. The

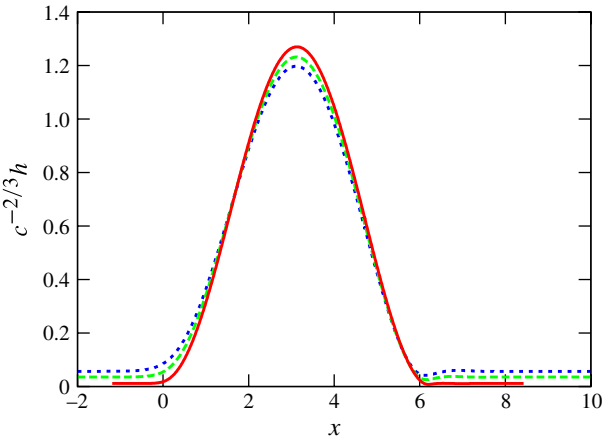

FIGURE 4. (Colour online) The main drop. The shape $h(x)$ obtained numerically scaled by $c^{2/3}$ for $G = 0.62$ dotted, 0.61 dashed and 0.60 continuous curves.

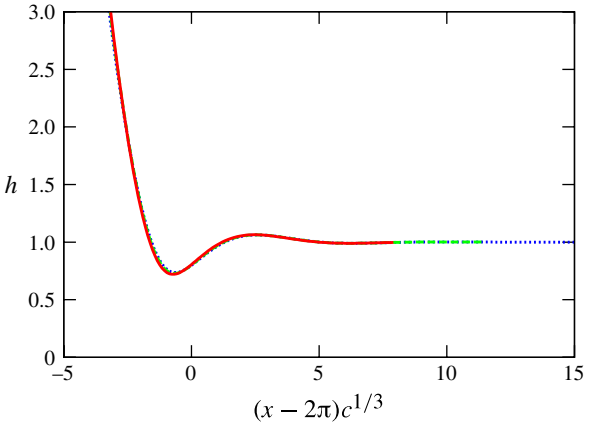

FIGURE 5. (Colour online) The right transition region. The shape h obtained numerically plotted as a function of the stretched variable $\xi = (x - 2\pi)c^{1/3}$ for $G = 0.62$ dotted, 0.61 dashed and 0.60 continuous curves.

small linear variation from -17.5 is due to gravity and we will look at this in more detail in the next paragraph. Without any contribution from the pressure gradient, the flux of liquid in the thin film would vary as $-ch + Gh^3$ in a frame moving with the wave. The pressure gradient keeps the flux equal to $-c + G$, its value in the uniform films. In the main drop where h is large, a very small pressure gradient is sufficient. However in the transition regions where $h = O(1)$ a large pressure gradient is required. This pressure gradient acts against the backward flux, so has a high pressure to the left and a low pressure to the right, in both transition regions. Hence we see in figure 6 the pressure dropping from -1 in the left-hand uniform film to the roughly constant value of -17.5 in the interior and then dropping again to a minimum of -25 where $h \approx 1$. Where $h < 1$ in the right-hand transition region, the pressure gradient reverses sign in

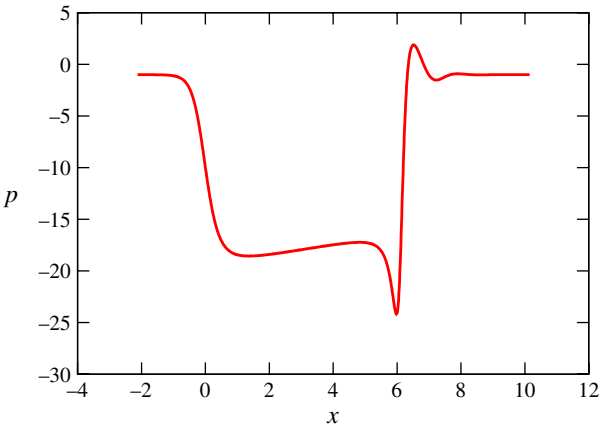

FIGURE 6. (Colour online) The variation of the capillary pressure in the solitary wave for $G = 0.61$.

order to add to the backward flux. This makes the pressure rise to a positive maximum, where again $h \approx 1$, before approaching the uniform value -1 in an oscillatory fashion.

In the matching region between the transition region and the main drop, the shape is parabolic

$$h \sim \tfrac{1}{2}P\xi^2 + R_\pm = \tfrac{1}{2}Pc^{2/3}(x - x_0)^2 + R_\pm. \tag{4.8}$$

The terms $R_\pm$ can be thought of as the effective thickness of the uniform films seen from within the large drop, respectively before and ahead of the drop. A large value of R_+ corresponds to a lower capillary pressure at the left-hand side, or top of the drop. The difference in pressure between the top and bottom of the drop is of course the hydrostatic pressure gradient G multiplied by the height difference 2π. Thus we conclude that

$$R_+ - R_- = 2\pi G, \tag{4.9}$$

which gives an estimate of $G \sim 0.5960$ for large solitary waves. This value is the critical value below which there are no steady solitary waves. The value corresponds to Kalliadasis & Chang's $\beta_c = 1.413 = G^{-2/3}$.

This concludes the first approximations, which have yielded the critical value of G and a relation between the speed c and the amplitude h_{max}. At this stage we have not determined how the speed depends on how close G is to its critical value. We need to proceed to corrections to the first approximations, and for this we must be more organized and follow Kalliadasis & Chang (1994) by making formal asymptotic expansions in a small parameter, matching different expansions in the transition regions and in the main drop.

5. Transition regions

Although the control parameter for the problem is the reduced Bond number G and the unknown is the speed c of the solitary wave, it is more convenient to find G in terms of an expansion in the small parameter $c^{-1/3}$, the same small parameter used by

Kalliadasis & Chang (1994). Thus we pose

$$G(c) \sim G_0 + c^{-1/3}0 + c^{-2/3}G_2 + c^{-1}G_3. \tag{5.1}$$

We have found already from the first approximations the critical value of G below which there are no steady solitary waves, $G_0 = 0.5960$. We shall find shortly that there is no need for an $O(c^{-1/3})$ correction.

With the rescaling $\xi = c^{1/3}(x - x_0)$, equation (2.5) governing the solitary wave becomes

$$h_{\xi\xi\xi} = \frac{h-1}{h^3} - c^{-2/3}h_\xi + c^{-1}G\frac{1-h^3}{h^3}. \tag{5.2}$$

This suggests an expansion

$$h \sim h_0 + c^{-1/3}0 + c^{-2/3}h_2 + c^{-1}h_3 + c^{-4/3}h_4 + c^{-5/3}h_5, \tag{5.3}$$

i.e. there appears to be no need for an $O(c^{-1/3})$ correction.

5.1. *The leading-order h_0*

The leading term h_0 is governed by the Bretherton equation

$$h_0''' = \frac{h_0 - 1}{h_0^3}, \tag{5.4}$$

where the prime denotes differentiation with respect to ξ. As h becomes large where the transition region merges with the main drop,

$$h_0 \sim \frac{1}{2}P\xi^2 + R_\pm - \frac{2}{3P^2}\xi^{-1} + \frac{2(1+2R_\pm)}{15P^3}\xi^{-3}. \tag{5.5}$$

The first two terms were discussed earlier. The correction terms were used when fitting to the numerical solution in order to extract accurate values of P and $R_\pm$. Fitting was performed with ξ in three ranges, (70, 120), (100, 150) and (120, 170), safely yielding four significant decimal places.

5.2. *The first correction h_2*

At leading order in the transition region, the capillary pressure is dominated by the curvature along the axis, i.e. the term $-h_{xx}$. The curvature around the axis, i.e. the term $-h$, drives the first correction to the shape in the transition region, through the last term in the equation

$$h_2''' = \frac{3 - 2h_0}{h_0^4}h_2 - h_0'. \tag{5.6}$$

This must be solved numerically. The asymptotic behaviour as the transition region merges into the main drop is

$$h_2 \sim -\frac{1}{4!}P\xi^4 + \frac{1}{2}a_{2\pm}\xi^2 + b_{2\pm}\xi + c_{2\pm} + \frac{8R_\pm + 4 + 20a_{2\pm}}{15P^3}\xi^{-1}. \tag{5.7}$$

In anticipation of the matching, one can adjust the free parameters in the far fields to make the linear terms $b_{2\pm}\xi$ vanish and to make the two coefficients of the quadratic terms equal, $a_{2-} = a_{2+}$. One then finds $a_2 = -1.220$, $c_{2+} = -1.33$ and $c_{2-} = -3.41$. Fitting the numerical solution to the asymptotic form was performed with ξ in three ranges, (30, 50), (40, 60) and (50, 70). It is difficult to obtain more accurate

numbers because h_1 becomes dominated by the large $-P\xi^4/4!$ term. Kalliadasis & Chang (1994) studied a scaled version of our equation for h_2 and numerically found $a_2 = -1.228$; our a_2 equals their $2d_2^{\pm}/\beta_c - a_0^{\pm}$, with their $2d_2^{+} = 2.357$, $2d_2^{-} = -2.926$, $\beta_c = 1.413$, $a_0^{+} = 2.897$ and $a_0^{-} = -0.842$.

5.3. *The second correction h_3*

While the motion of the drop is eventually driven by gravity, G first appears in the $O(c^{-1})$ correction of the transition regions. This correction is governed by

$$h_3''' = \frac{3-2h_0}{h_0^4}h_3 - G_0\left(1-\frac{1}{h_0^3}\right). \tag{5.8}$$

The asymptotic behaviour as the transition region merges into the main drop is

$$h_3 \sim -\frac{1}{3!}G_0\xi^3 + \frac{1}{2}a_{3\pm}\xi^2 + b_{3\pm}\xi + \frac{4G_0}{3P^3}\log\xi + c_{3\pm} + \frac{4a_{3\pm}}{3P^3}\xi^{-1}. \tag{5.9}$$

Again one can adjust the free parameters in the far fields to make the linear terms $b_{3\pm}\xi$ vanish and to make the two coefficients of the quadratic terms equal, $a_{3-} = a_{3+}$. One then finds $a_3 = -0.1452$, $c_{3+} = 0.2$ and $c_{3-} = -1.0$. Fitting the numerical solution to the asymptotic form was performed with ξ in two ranges, (30, 50) and (40, 60). The presence of the $\log\xi$ term will require an $O(c^{-1}\log c)$ term in the expansion of h in the main drop.

5.4. *The third correction h_4*

This correction to h_2 is only required to catch all the terms in the matching of the asymptotic expansions. It is forced in the following equation by the curvature along the fibre in h_2 in the same way as h_2 itself was forced by the curvature along the fibre in h_0:

$$h_4''' = \frac{(3-2h_0)}{h_0^4}h_4 + \frac{3(h_0-2)h_2^2}{h_0^5} - h_2'. \tag{5.10}$$

To the resolution required, the asymptotic behaviour as the transition region merges into the main drop is

$$h_4 \sim \frac{1}{6!}P\xi^6 - \frac{1}{4!}a_2\xi^4 + \frac{11}{1080P^2}\xi^3 + \frac{1}{2}a_{4\pm}\xi^2. \tag{5.11}$$

It is thought that a_4 may be around 0.8, although seeing this term behind the much larger terms in the asymptotic behaviour is difficult.

6. Main drop

We have seen in the first approximations that in the main drop h is $O(c^{2/3})$. We therefore write $h = c^{2/3}H$, so that the governing equation (2.5) becomes

$$(H + H_{xx})_x = -c^{-2/3}G_0 + c^{-1}\frac{1}{H^2} - c^{-4/3}G_2 - c^{-5/3}\left(G_3 + \frac{1}{H^3}\right) + c^{-8/3}\frac{G_0}{H^3}. \tag{6.1}$$

This suggests an expansion

$$H \sim H_0 + c^{-1/3}0 + c^{-2/3}H_2 + c^{-1}H_3 + c^{-4/3}H_4 + (c^{-5/3}\log c)H_{5\ell} + c^{-5/3}H_5. \tag{6.2}$$

The $c^{-5/3}\log c$ term is triggered by the $\log\xi$ term in h_3 in the transition regions and hence denoted by the subscript ℓ.

6.1. *The leading-order H_0*

In the first approximations, we have already found the leading-order term in the main drop

$$H_0 = P(1-\cos x). \tag{6.3}$$

Because h is large, it must vanish at the transition regions in order to become $O(1)$ there. The solution has a large constant capillary pressure $-c^{2/3}P$.

6.2. *The first correction H_2*

The first correction contains the hydrostatic pressure gradient. It is governed by

$$H_2' + H_2''' = -G_0, \tag{6.4}$$

where the prime denotes differentiation with respect to x. It has the solution

$$H_2 = G_0(\sin x - x) + A_2 + C_2(1-\cos x) \tag{6.5}$$

with constants A_2 and C_2 to be found by matching. In anticipation of the matching, we have assumed that H_2' vanishes at the ends $x=0$ and 2π.

6.3. *The second correction H_3*

In the second correction, a pressure gradient drives a viscous flow which cancels the unscaled flux ch. The correction is governed by

$$H_0^3(H_3 + H_3'')' = H_0. \tag{6.6}$$

It has a solution

$$H_3 = -\frac{\sin x}{3P^2(1-\cos x)} + A_3 + B_3\sin x + C_3(1-\cos x), \tag{6.7}$$

with constants A_3, B_3 and C_3 to be found by matching. The existence of this closed-form expression aids the detailed matching. As $x\to x_0$, with $x_0=0$ for the left-hand transition region and $x_0=2\pi$ for the right-hand transition,

$$H_3 = -\frac{2}{3P^2}(x-x_0)^{-1} + A_3 + O(x-x_0). \tag{6.8}$$

The singular first term will match the decaying third term in h_0, (5.5). The fact that the constant term is the same, A_3, at both ends of the main drop means that there is no need for a $c^{-1/3}G_1$ term in the expansion of the reduced Bond number in (5.1).

6.4. *The third correction H_4*

The third correction is a copy of the first correction H_1 and is forced by the difference in the value of G from its critical value G_0. This difference will eventually give the first approximation to how the speed c depends on G. The third correction is governed by an equation similar to that for H_2:

$$H_4' + H_4''' = -G_2, \tag{6.9}$$

and has the solution

$$H_4 = G_2(\sin x - x) + A_4 + B_4 \sin x + C_4(1 - \cos x), \tag{6.10}$$

with constants A_4, B_4 and C_4 to be found by matching.

6.5. *The fourth correction* $H_{5\ell}$

The fourth correction, and $\log c$ term, is not forced by the interior of the main drop but by matching, and so is relatively straightforward. It is governed by

$$H'_{5\ell} + H'''_{5\ell} = 0, \tag{6.11}$$

with solution

$$H_{5\ell} = A_{5\ell} + B_{5\ell} \sin x + C_{5\ell}(1 - \cos x), \tag{6.12}$$

with constants $A_{5\ell}$, $B_{5\ell}$ and $C_{5\ell}$ to be found by matching.

6.6. *The fifth correction* H_5

The fifth correction is forced by a second adjustment in the value of G, by the correction by H_2 to the forcing of H_3, and by a new term $1/H_0^3$:

$$H'_5 + H'''_5 = -G_3 - \frac{2H_2}{H_0^3} - \frac{1}{H_0^3}. \tag{6.13}$$

The solution is given by

$$\begin{aligned} H_5 = \frac{1}{15P^3} \Bigg[& \frac{\left(\frac{1}{2} + A_2 - G_0 x\right) \sin x}{(1 - \cos x)^2} + 2\frac{(1 + 2A_2 + 5C_2 - 2G_0 x) \sin x + G_0}{(1 - \cos x)} \\ & + 4G_0(2 + 3\cos x) \ln\left(2 \sin \frac{1}{2}x\right) + 15G_0 \cos x \\ & - 2(3A_2 + 10C_2 - 3G_0 x) \sin x - \frac{22}{3} G_0 \Bigg] \\ & - G_3(x - \sin x) + A_5 + B_5 \sin x + C_5(1 - \cos x). \end{aligned} \tag{6.14}$$

The most important term is the gravitational contribution $-G_3 x$ on the last line; all the other terms will match contributions from the transition region.

7. Matching

At the level of approximations considered, the transition regions are fully determined, while the main drop has a number of as yet undetermined constants, the A_n, B_n and C_n, as well as the important coefficients G_n in the expansion of G. To match the expansion for the left-hand transition region as $\xi \to \infty$ to that for the main drop as $x \to 0$, we express the two asymptotic expansions in terms of $x = \xi c^{-1/3}$ and collect terms of the same order in $c^{-n/3}$. The behaviour of the left-hand transition

region is

$$\begin{array}{lllll}
 & h_0 & h_2 & h_3 & h_4 \\
c^{2/3}\Big[& \frac{P}{2}x^2 & -\frac{P}{4!}x^4 & & +\frac{P}{6!}x^6 \quad +\cdots\Big] \\
+c^{0}\Big[& R_+ & +\frac{a_2}{2}x^2 & -\frac{G_0}{3!}x^3 & -\frac{a_2}{4!}x^4 \quad +\cdots\Big] \\
+c^{-1/3}\Big[& -\frac{2}{3P^2x} & & +\frac{a_3}{2}x^2 & +11k_4x^3 \quad +\cdots\Big] \\
+c^{-2/3}\Big[& & +c_{2+} & & +\frac{a_4}{2}x^2 \quad +\cdots\Big] \\
+c^{-1}\log c\Big[& & & +\frac{1}{3}k_3 & +\cdots\Big] \\
+c^{-1}\Big[& \frac{k_1}{x^3} & +\frac{k_2}{x} & +k_3\log x + c_{3+} & +\cdots\Big],
\end{array} \tag{7.1}$$

where $k_1 = 2(1 + 2R_+)/15P^3$, $k_2 = 4(1 + 2R_+ + 5a_2)/15P^3$, $k_3 = 4G_0/3P^3$ and $k_4 = 1/1080P^2$. The columns give the contributions from the different terms $c^{-n/3}h_n$, while the rows give terms of the same order in $c^{-n/3}$. The expansion for the left-hand transition region is the same for the right-hand transition region, except that the $+$ subscripts are replaced by $-$ subscripts and x is replaced by $x - 2\pi$.

The behaviour of the main drop is

$$\begin{aligned}
& c^{2/3}\ \left[\frac{P}{2}x^2 - \frac{P}{4!}x^4 + \frac{P}{6!}x^6 + \cdots\right] \\
& +c^{0}\ \left[-G_0x_0 + A_2 + \frac{C_2}{2}x^2 - \frac{G_0}{3!}x^3 - \frac{C_2}{4!}x^4 + \cdots\right] \\
& +c^{-1/3}\ \left[-\frac{2}{3P^2x} + A_3 + \left(\frac{1}{18P^2} + B_3\right)x + \frac{C_3}{2}x^2 + \left(k_4 - \frac{B_3}{3!}\right)x^3 \ldots\right] \\
& +c^{-2/3}\ \left[-G_2x_0 + A_4 + B_4x + \frac{C_4}{2}x^2 + \cdots\right] \\
& +c^{-1}\log c\ \ [A_{5\ell} + \cdots] \\
& +c^{-1}\ \left[\frac{k_5}{x^3} + \frac{k_6}{x} + k_3\log x - G_3x_0 + A_5 \ldots\right],
\end{aligned} \tag{7.2}$$

with the previous k_3 and k_4 and with new $k_5 = 2(1 + 2A_2 - 2G_0x_0)/15P^3$ and $k_6 = 4(1 + 2A_2 + 5C_2 - 2G_0x_0)/15P^3$. The rows come from the different H_n. The expansion above is for the left-hand end of the main drop around $x = 0$ with $x_0 = 0$. There is the same expansion around the right-hand end, with all the x replaced by $(x - x_0)$ and with $x_0 = 2\pi$.

(*a*) Matching at $O(c^{2/3})$ is successful with the same three powers of x present with the same coefficients. This is a consequence of the first approximations setting the calculation off in the correct direction.

(*b*) Matching at $O(c^0)$ gives from the constant terms $A_2 = R_+$ from the left-hand transition and from the right-hand transition $-2\pi G_0 + A_2 = R_-$. This gives the critical value of the reduced Bond number $G_0 = (R_+ - R_-)/2\pi = 0.5960$ as well as $A_2 = 2.8996$. The x^2- and x^4-terms both give $C_2 = a_2 = -1.220$. The x^3-terms have the same coefficient.

(*c*) Matching at $O(c^{-1/3})$ the x^{-1}-terms have the same coefficient, while the constant terms give $A_3 = 0$. The x-terms give $B_3 = -1/18P^2 = -0.1344$, while the x^2-terms give $C_3 = a_3 = -0.1452$. Finally the x^3-terms give $11k_4 = k_4 - B_3/6$, i.e. $B_3 = -60k_4 = -1/18P^2$ again.

(*d*) Matching at $O(c^{-2/3})$ gives from the constant terms $A_4 = c_{2+}$ from the left-hand transition and from the right-hand transition $-2\pi G_2 + A_4 = c_{2-}$. This gives the first correction to the reduced Bond number $G_2 = (c_{2+} - c_{2-})/2\pi = 0.33$ as well as $A_4 = -1.33$. The x-terms give $B_4 = 0$, while the x^2-terms give $C_4 = a_4 = 0.8$.

(*e*) Matching at $O(c^{-1}\log c)$ gives from the constant terms $A_{5\ell} = \frac{1}{3}k_3 = 4G_0/9P^3 = 0.9964$.

(*f*) Matching at $O(c^{-1})$ the x^{-3}-terms are the same by $R_\pm = A_2 - G_0 x_0$. The x^{-1}-terms are the same by $R_\pm = A_2 - G_0 x_0$ and $a_2 = C_2$. The $\log x$-terms have the same coefficients. The constant terms give $A_5 = c_{3+}$ from the left-hand transition and $-2\pi G_3 + A_5 = c_{3-}$ from the right-hand transition. This gives the second correction to the reduced Bond number $G_3 = (c_{3+} - c_{3-})/2\pi = 0.19$ and $A_5 = 0.20$.

All the terms in the asymptotic expansions for the main drop and for the transition regions have matched successfully. The matching process has determined the free coefficients in the main drop as follows:

$$\left.\begin{array}{lll} A_2 = 2.8998 & & C_2 = -1.220 \\ A_3 = 0 & B_3 = -0.1344 & C_3 = -0.1452 \\ A_4 = -1.33 & B_4 = 0 & C_4 = 0.8 \\ A_{5\ell} = 0.9964 & & \\ A_5 = 0.2 & & \end{array}\right\} \tag{7.3}$$

With many terms for the shape of the drop now determined, we can refine the prediction made in § 4 for the maximum displacement. The maximum occurs within $O(c^{-2/3})$ of $x = \pi$, so to $O(c^{-1/3})$ we can just evaluate h at $x = \pi$. We thus predict the maximum

$$h_{max} = 2Pc^{2/3} + (-G_0\pi + A_2 + 2C_2) + (A_3 + 2C_3)c^{1/3} + O(c^{-2/3}), \tag{7.4}$$

i.e.

$$h_{max} = 1.2860c^{2/3} - 1.413 - 0.2904c^{-1/3} + O(c^{-2/3}). \tag{7.5}$$

For the three solitary waves in figure 4 with $G = 0.62$, 0.61 and 0.60, we found in § 4 that $h(\pi) - 2Pc^{2/3} = -1.497$, -1.473 and -1.443 using the computed value of the

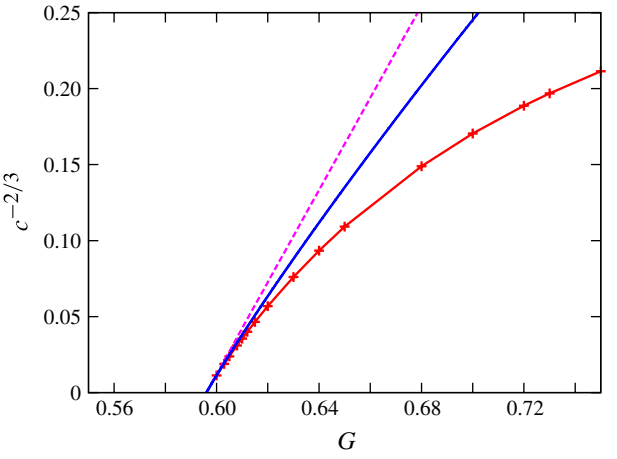

FIGURE 7. (Colour online) The speed c as a function of the reduced Bond number G. The line with points is the numerical solution, the dashed line corresponds to the first two terms in (7.6), while the continuous line corresponds to all three terms.

speed c. The refined prediction $-1.413 - 0.2904c^{-1/3}$ for these three waves is -1.482, -1.468 and -1.444.

Collecting together the results for the G_n, we have an expansion for the reduced Bond number G in terms of the small parameter $c^{-1/3}$,

$$G = 0.5960 + 0.33c^{-2/3} + 0.19c^{-1} + O(c^{-4/3}). \tag{7.6}$$

In figure 7 we test this asymptotic prediction of $G(c)$ against numerical solutions of the governing equation. We have chosen to follow figure 3 and give the results as a function of G, and we have chosen to plot $c^{-2/3}$ in place of c because we are interested in the limit $c \to \infty$. The first two terms of (7.6) give c within a 10 % error once $c > 755$, while the three terms together give the same accuracy once $c > 135$.

At the end of § 4, we found that the terms $R_\pm$ leaving the transition region could be thought of as a difference in the capillary pressure $(R_+ - R_-)$ between the top and bottom of the large drop. This pressure difference was balanced by a hydrostatic pressure difference $2\pi G_0$, which was independent of the speed c. The correction h_2 to the transition region, which is forced by the curvature around the axis in h_0, produces an additional pressure difference $(c_{2+} - c_{2-})c^{-2/3}$. There is a further pressure drop $(c_{3+} - c_{3-})c^{-1}$ from h_3 which is forced by G_0 in the transition region. These additional pressure drops, which do depend on the speed, require a corresponding additional hydrostatic pressure drop, i.e.

$$2\pi G \sim (R_+ - R_-) + (c_{2+} - c_{2-})c^{-2/3} + (c_{3+} - c_{3-})c^{-1}. \tag{7.7}$$

To this level of approximation, gravity is only providing a pressure difference across the main drop to balance the different pressure differences across the advancing right-hand transition region and the retreating left-hand transition region. Curiously there is no $G_1 c^{-1/3}$ term. Such a term would have been required for the viscous pressure gradient in the main drop, as is calculated in H_3, had there been a different constant term at its two ends.

8. Discussion

The problem studied in this paper has required the calculation of an unusually large number of correction terms before finding a leading-order description of the motion of the large drop. The first approximations of H_0 in the main drop and h_0 in the thin transition regions yielded information about the shape, which was tested in figures 4 and 5, and yielded a relation between the speed c and the amplitude, $h_{max} = 2Pc^{2/3}$. Gravity first entered in the correction H_2, and this yielded the value of the critical reduced Bond number G_0. Thus at this level of approximation the speed was unknown. One might have expected that the viscous pressure gradient in the correction H_3 to the main drop would relate the speed to how much G exceeded its critical value, but fortuitously we found $G_1 = 0$. It was only through the correction h_2 in the transition regions with the third correction H_4 in the main drop that c was first related to $G - G_0$. Thus the control of the speed depends on Bretherton's transition regions being corrected for the small effect of the curvature around the axis. Our additional terms h_3 and H_5 enabled us to find the first correction to the relation between c and $G - G_0$, as plotted in figure 7. For technical reasons, these additional terms h_3 and H_5 required consideration of h_4 and $H_{5\ell}$.

Our calculation does not fully agree with that of Kalliadasis & Chang (1994). We agree on the leading order in the main drop (our H_0, their Φ_0) and in the transition region (our h_0, their H_0). We agree on much of the first correction in the two regions (our H_2 and h_2, their Φ_2 and H_2), including the critical value of a non-dimensional group (our $G_0 = 0.5960$, their $\beta_c = 1.413 = G_0^{-2/3}$). We disagree on higher corrections and on the dependence of the speed on the difference of the non-dimensional group from its critical value (our $G = G_0 + 0.33c^{-2/3}$, their $\beta = \beta_c - 4.2c^{-1}$). A direct comparison between the two calculations is complicated by our choice of a different non-dimensionalization; we scale the axial distance with the radius of the fibre, they use a reduced capillary length. We will return to the issue of this choice shortly.

To find the first approximation between the speed and the non-dimensional group, we found it necessary to go to the third non-trivial correction $c^{-4/3}H_4$ in the main drop. Kalliadasis & Chang found only one part of the second correction, their Φ_3 for which they solved their simplified equation (75) rather than their full equation (53*d*), and did not go to the third correction.

To match the main drop to the transition regions, we have displayed the full functional form of the two asymptotic approximations in the matching zone. On the other hand Kalliadasis & Chang just equated the value of the function and the value of several derivatives at a single point, at their $z^{\pm} = \pm\pi\beta_c^{-1/2}$. If the behaviour in the matching zone were a low-order polynomial, their matching strategy would have worked. We however have found that at the level of the second correction, that is before the level which determines the speed, there is an inverse power which causes problems in their strategy. And at the level of the fifth correction, we find x^{-3} terms and logarithms. Because Kalliadasis & Chang did not find all of their second correction in the main drop, Φ_3, they did not see the x^{-1} singular behaviour as the ends are approached. Because Kalliadasis & Chang did not look at the decay of the leading-order transition term to its parabolic form, they did not see the term available to match this singular behaviour.

Turning now to the choice of non-dimensionalization, there is what appears a small superficial difference between our form for the main drop $H_0 = P(1 - \cos x)$ and their $\Phi_0 = (2d_0/\beta_c)(1 + \cos(\beta_c^{1/2}z))$. Note that the length of our main drop is 2π while theirs is $2\pi\beta_c^{-1/2}$, and therein is hidden a problem. In our non-dimensionalization,

we have to find the strength of gravity G to generate the required hydrostatic pressure difference between the top and the bottom of the drop. In Kalliadasis & Chang's non-dimensionalization, they effectively have a fixed magnitude of gravity and have to find the length of the drop, $2\pi\beta^{-1/2}$, which generates the required pressure difference across it. In other words, Kalliadasis & Chang should be finding the small change in the length as their control parameter changes from β_c to β, which would require moving the matching point from $z^{\pm} = \pm\pi\beta_c^{-1/2}$ by a small $c^{-2/3}$ amount to be determined. It is probable that the failure to recognize this issue and introduce the extra degree of freedom in the unknown small increase in length lead to their erroneous expression for the speed.

REFERENCES

BRETHERTON, F. P. 1961 The motion of long bubbles in tubes. *J. Fluid Mech.* **10**, 166–188.

CHANG, H.-C. & DEMEKHIN, E. A. 1999 Mechanism for drop formation on a coated vertical fibre. *J. Fluid Mech.* **380**, 233–255.

CRASTER, R. V. & MATAR, O. K. 2006 On viscous beads flowing down a vertical fibre. *J. Fluid Mech.* **553**, 85–105.

DUPRAT, C., RUYER-QUIL, C., KALLIADASIS, S. & GIORGIUTTI-DAUPHINÉ, F. 2007 Absolute and convective instabilities of a viscous film flowing down a vertical fibre. *Phys. Rev. Lett.* **98**, 244502.

HAMMOND, P. S. 1983 Nonlinear adjustment of a thin annular film of a viscous fluid surrounding a thread of another within a circular pipe. *J. Fluid Mech.* **137**, 363–384.

KALLIADASIS, S. & CHANG, H.-C. 1994 Drop formation during coating of vertical fibres. *J. Fluid Mech.* **261**, 135–168.

KLIAKHANDLER, I. L., DAVIS, S. H. & BANKOFF, S. G. 2001 Viscous beads on vertical fibre. *J. Fluid Mech.* **429**, 381–390.

QUÉRÉ, D. 1990 Thin films flowing on vertical fibres. *Europhys. Lett.* **13**, 721–726.

SMOLKA, L. B., NORTH, J. & GUERRA, B. K. 2008 Dynamics of free surface perturbations along an annular viscous film. *Phys. Rev.* E **77**, 036301.